

# Efficient Loading and Controlled Release of Benzophenone-3 Entrapped Into Self-Assembling Nanogels

Samia Daoud-Mahammed<sup>#</sup>, Sunil A. Agnihotri<sup>#</sup>, Kawthar Bouchemal, Stefanie Klötters, Patrick Couvreur and Ruxandra Gref<sup>\*#</sup>

Université Paris-Sud 11, UMR CNRS 8612. Faculté de Pharmacie, 5, Rue J.B. Clément. 92296 Châtenay Malabry, France

**Abstract:** Benzophenone-3 (BZ-3), was successfully entrapped into nanogels prepared by a simple one-step method based on self-assembly of two water soluble polymers: a hydrophobically modified dextran (MD) and a  $\beta$ -Cyclodextrin polymer ( $\beta\beta$ -CD). Isothermal titration microcalorimetry (ITC) and phase solubility experiments were performed at 4, 25 or 37°C to investigate the interaction of the hydrophobic BZ-3 with MD and  $\beta\beta$ -CD. The BZ-3 entrapment efficiency, yield of nanogels formation, particle size, and BZ-3 release were also evaluated. BZ-3/ $\beta\beta$ -CD interaction was characterized by association constants  $K=5180\text{ M}^{-1}$  and  $K'=2700\text{ M}^{-1}$ , as determined by phase solubility and ITC experiments, respectively. Differences obtained in association constants values were discussed critically. Results indicate that both  $K$  and  $K'$  decrease with increase in temperature. The strong interactions between BZ-3 and  $\beta\beta$ -CD were characterized by a negative enthalpy change ( $\Delta H$ ) with entropic contribution ( $T\Delta S$ ). Monodisperse nanogels were produced with an entrapment up to 75 % and yield up 84 %. BZ-3 was firmly entrapped into nanogels, as only the dilution of the nanogels led to its release. This system provides an advantage for sunscreen formulation to prevent systemic penetration of BZ-3. The 'green' (solvent free) preparation method, and the possibility of unlimited storage after freeze drying makes these nanogels valuable candidates for the entrapment of sun screen agents.

**Keywords:** Nanogels, cyclodextrins, inclusion complexes, sunscreen, isothermal titration microcalorimetry, drug loading.

## 1. INTRODUCTION

Benzophenone-3 (BZ-3), chemically known as 2-hydroxy-4-methoxybenzophenone (Fig. 1A), is used in a variety of consumer products for its capacity to absorb and dissipate ultraviolet radiations [1-3]. Because BZ-3 protects the skin from harmful UV-A rays (320-400 nm) and enhances UV-B (290-320 nm) protection of other sunscreen agents (homosalate, octyl salicylate, OM-cinnamate, octinoxate, etc), BZ-3 is most often used in conjunction with these products. Furthermore, by absorbing UV rays, BZ-3 also helps to prevent the integrity of other cosmetic ingredients from deteriorating under the sun and helps to stabilize complex formulations and color cosmetics. Consequently, BZ-3 is widely used in a variety of personal care products such as nail polish, sunscreen lotions/creams, lip care products, shampoo, and fragrances.

The efficacy of sunscreen formulations depend on low UV penetration profiles and high photoprotection. These characteristics are important for cosmetic sunscreen safety. Successful development of BZ-3 formulations encounters following two major challenges. Firstly, despite of its sun protective ability, BZ-3 has been shown to penetrate the skin and cause photo-sensitivity [1, 4-8]. It has also been suspected to cause contact eczema [9] and is believed to be a contributing factor in the recent rise of Melanoma cases with sunscreen users [10]. Some studies have also shown that BZ-3 behaves similar to the hormone estrogen, suggesting that it may cause breast cancer [11, 12]. Therefore, there is an urgent need to develop cosmetic formulations preventing BZ-3 skin penetration. Secondly, BZ-3 is poorly soluble in water (about 0.25 mM at 25°C) which poses a serious concern for the development of efficient formulations.

Various strategies to reduce the systemic uptake of drugs by targeting the molecules to the upper layers of the skin have been investigated. Jiang *et al.* reported that increasing the solubility of BZ-3 in the vehicle reduced the thermodynamic activity of the solute in the vehicle, thereby decreasing solute availability from the

vehicle and leading to reduced permeability [13]. One of the strategies for increasing apparent water solubility is the complexation with cyclodextrins (CDs) [14-17]. CDs have been recognized in the cosmetic field as potent carriers for the formulation of poorly water-soluble molecules [18]. CDs are cyclic oligosaccharides consisting of six to eight D-glucopyranose units linked through  $\alpha$ -1,4-glycosidic bonds. They have the shape of a truncated cone with a hydrophobic internal cavity surrounded by an external hydrophilic surface. This particular structure enables CDs to accommodate into their cavity a wide variety of hydrophobic molecules, thereby modifying their physico-chemical properties [14, 15, 19]. The inclusion of the "guest" molecule into the "host" CD can improve its apparent solubility, physical and chemical stability, dissolution and bioavailability, reduce its toxicity, thus making CDs very attractive in drug delivery and formulation.

Recently, our group has proposed a mild procedure to obtain colloidal nanoassemblies (nanogels) containing CDs in the absence of organic solvents [20]. Spherical shaped nanogels of 100-200 nm are formed spontaneously in aqueous medium upon the association of two water soluble polymers: a hydrophobically modified dextran (MD) (obtained by grafting alkyl side chains to the dextran backbone) and a  $\beta$ -cyclodextrin ( $\beta$ -CD) polymer ( $\beta\beta$ -CD) (obtained by crosslinking  $\beta$ -CD) (Fig. 1B). The MD alkyl chains form inclusion complexes with some CD cavities, leaving a large majority of CDs available to include other hydrophobic molecules of interest. It was our aim here to take advantage of this particularity to include BZ-3 in self-assembling nanogels.

Isothermal titration microcalorimetry (ITC) is a modern and sensitive method available for the determination of thermodynamics of the host (CD)-guest interaction [21-30]. ITC shows whether an association process occurs and allows the evaluation of the association constant ( $K$ ), the enthalpy ( $\Delta H$ ) and the entropy ( $\Delta S$ ) changes of the interaction from which the Gibbs free energy ( $\Delta G$ ) of the process can be derived [21, 27, 31, 32].

In the present study, ITC has been used in conjunction with phase solubility studies to gain information on the inclusion ability of  $\beta\beta$ -CD toward the hydrophobic sunscreen BZ-3, in comparison with that of native  $\beta$ -CD. As the temperature is a well known parameter that could modify the stability of inclusion complexes, a

\*Address correspondence to this author at the UMR CNRS 8612, School of Pharmacy, 5 Rue J.B. Clément, 92290 Châtenay Malabry, France; Tel: (33) 1 46 83 59 09; Fax:?????????; E-mail: ruxandra.gref@u-psud.fr  
<sup>#</sup>equally contributing authors

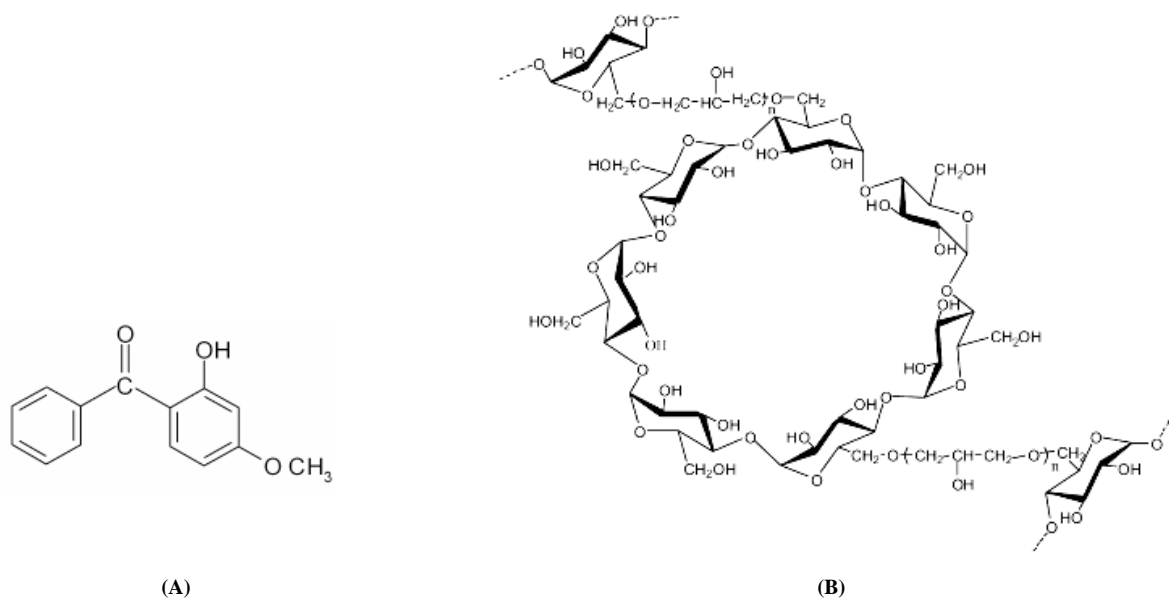


**Fig. (1).** Chemical structure of (A) Benzophenone-3 and (B) Poly- $\beta$ -Cyclodextrin.

special attention was brought to the effect of temperature on BZ-3/CDs interactions, especially between 4°C and 37°C, which are consistent with storage and customary temperatures.

We further took advantage of these interactions to formulate BZ-3 loaded MD/p $\beta$ -CD nanogels (nanoassemblies). Finally, the stability of the nanogels suspension as well as the effect of dilution and temperature on the release of BZ-3 was investigated.

## 2. MATERIALS AND METHODS

### 2.1. Materials

$\beta$ -cyclodextrin polymer (p $\beta$ -CD) was prepared by crosslinking  $\beta$ -cyclodextrin ( $\beta$ -CD) with epichlorohydrin (EP), under strong alkaline conditions. Briefly, 100g of anhydrous  $\beta$ -CD was dissolved in 160mL NaOH (33% w/w) solution under mechanical stirring overnight. Then, 81.52g of EP (molar ratio  $\beta$ -CD/EP = 10) was rapidly added to the solution heated to 30°C. In order to obtain soluble polymer with high molar masses (M), the reaction was stopped in the vicinity of gelation point by addition of acetone. The obtained aqueous phase was heated overnight at 50°C, neutralized with 6N HCl and ultrafiltered using membranes with a cut-off of 100,000 g/mol. The p $\beta$ -CD polymer was finally recovered by freeze-drying. The  $\beta$ -CD content in p $\beta$ -CD was 70% w/w, according to the  $^1\text{H}$  NMR spectra. The average molar mass of p $\beta$ -CD polymer was  $7 \times 10^5$  g/mol, as determined by size exclusion chromatography using pollutant standards.

To synthesize dextran bearing hydrophobic lauryl side chains (MD), 4g of dextran (40,000 g/mol) was solubilized in 100 mL of dimethyl formamide containing 1g of lithium chloride. Then, 0.43 mL of lauroyl chloride and 0.031 mL of pyridine were added to the dextran solution. The reaction was carried out at 80°C for 3 hours. The obtained MD was isolated by precipitation in isopropyl alcohol. It was further solubilized in distilled water, purified by dialysis for 48 hours and finally freeze-dried. The substitution yield of MD was 4.8 % of glucose units, as determined using  $^1\text{H}$  NMR spectroscopy.

BZ-3 was purchased from Sigma-Aldrich (France). Water was purified by reverse osmosis (Milli-Q<sup>®</sup>, Millipore Corporation, USA). All the chemicals used were of analytical grade.

## 2.2. Methods

### 2.2.1. Determination of BZ-3 Concentration

BZ-3 concentrations were determined by UV spectrophotometry at 290 nm (Perkin Elmer UV/VIS spectrophotometer, Germany). A calibration curve with correlation coefficient ( $r$ ) of 0.9983 was obtained. The assay has been validated and was reliable in the presence of cyclodextrins and MD polymer.

### 2.2.2. Solubilization Assays

To study the solubilisation of BZ-3 by using  $\beta$ -CD, p $\beta$ -CD and MD, a series of experiments were conducted:

- **Determination of the time Required to Reach the Equilibrium of BZ-3/CDs Complexation**

For this purpose, the kinetics of BZ-3 solubilization was studied by introducing  $\beta$ -CD or p $\beta$ -CD aqueous solutions (10 g/L or 50 g/L) into vials containing excess amounts of BZ-3 with regards to the solubility. The samples were protected from light and shaken at a controlled temperature of  $25 \pm 0.5^\circ\text{C}$ . At each time point (2, 4, 6, 8, 10, 12, 24 and 72 h), 1 mL of each solution was taken out, centrifuged ( $3000 \times g$ , 10 min) and then ultracentrifuged for 45 minutes at  $112,500 \times g$  (Beckman L7-55, USA) to remove the insoluble fraction of BZ-3. The concentration of solubilized BZ-3 was measured by UV spectrophotometry at 290 nm as previously described.

- **Phase Solubility Assays**

Phase solubility studies were performed according to the Higuchi and Connors method [33]. A series of p $\beta$ -CD aqueous solutions of increasing concentrations (0 - 300 g/L) were introduced into vials containing an excess amount of BZ-3. The suspensions were shielded from light and shaken at a controlled temperature of 25, 37 or  $4 \pm 0.5^\circ\text{C}$ . After equilibrium has been reached (12 hours), an aliquot of each sample was centrifuged ( $3000 \times g$ , 10 min) and then ultracentrifuged at 25, 37 or 4°C for 45 minutes at  $112,500 \times g$  (Beckman L7-55, USA) to obtain BZ-3 loaded p $\beta$ -CD solutions. The concentration of solubilized BZ-3 was measured by UV spectrophotometry as described previously. These studies were performed in triplicate for each of the samples.

The phase solubility diagrams were obtained by plotting the mean solubility of BZ-3 against  $\beta$ -CD concentrations. For p $\beta$ -CD,

the  $\beta$ -CD concentrations were calculated to be 70% w/w as estimated by  $^1\text{H}$  NMR spectroscopy.

The apparent stability constants ( $K_S$ ) of the BZ-3/ $\beta$ -CD complexes formed were calculated from the regression curve of the initial straight line of the solubility diagrams, with the assumption of a 1:1 stoichiometry, according to Eq. 1:

$$K_S = \frac{\text{slope}}{S_0(1 - \text{slope})} \quad \text{Eq. 1}$$

where,  $S_0$  is BZ-3 solubility in water, in the absence of  $\beta$ -CD.

#### • Solubilization of BZ-3 by $\beta$ -CD and MD

The solubilization of BZ-3 by the  $\beta$ -CD monomer and MD polymer was studied by using the same procedure as previously described for p $\beta$ -CD. The concentration of MD and  $\beta$ -CD solutions was increased up to 15g/L, close to the maximal solubility of  $\beta$ -CD in water (18.5 g/L) [34]. In the case of MD, the range of concentrations was in the order of magnitude with the one used for nanogel preparation.

#### 2.2.3. Preparation of Solutions for ITC Experiments

Before preparation of the solution for ITC experiments, the water content in each material ( $\beta$ -CD and p $\beta$ -CD) was accurately determined by weighting the samples before and after drying under vacuum at 105°C during 24 hours. Then, the water content was taken into account to determine the accurate amount of powder to be dissolved in water to reach the concentrations needed for ITC experiments.

- $\beta$ -CD (10 mM) and p $\beta$ -CD (concentration of  $\beta$ -CD cavities = 10 mM) solutions were prepared by dissolving the corresponding weight of  $\beta$ -CD and p $\beta$ -CD powder into MilliQ<sup>®</sup> water. Solutions were magnetically stirred overnight to ensure the complete solubilization of material.
- For the preparation of BZ-3 solutions, an excess of BZ-3 (25 mg) was placed in a glass vial together with 50 mL of MilliQ<sup>®</sup> water under magnetic stirring overnight at 25°C. The suspension was centrifuged (3000  $\times$ g, 10 min) and then ultracentrifuged for 45 minutes at 112,500  $\times$ g (Beckman L7-55, USA) to remove the insoluble BZ-3. After appropriate dilution with MilliQ<sup>®</sup> water, BZ-3 concentration in the solution was measured spectrophotometrically as described above.

#### 2.2.4. Isothermal Titration Microcalorimetry (ITC) Studies.

An isothermal calorimeter (ITC) (MicroCal Inc., USA) has been used for determining simultaneously from a single titration curve, the enthalpy of the interaction between BZ-3 and cyclodextrins in their native or polymerized form and equilibrium constants corresponding to the formation of a complex between those species. The ITC instrument was periodically calibrated either electrically using an internal electric heater, or chemically by measuring the dilution enthalpy of methanol in water. This standard reaction was in excellent agreement (1-2%) with MicroCal constructor data.

In a typical experiment, 10  $\mu\text{L}$  of  $\beta$ -cyclodextrin (10mM) or p $\beta$ -CD (concentration of  $\beta$ -CD cavities =10mM) aqueous solution contained into 283  $\mu\text{L}$  syringe, was used to titrate an aqueous solution of BZ-3 into the calorimetric cell. Intervals between injections were 600s and agitation speed was 220 rpm. A background titration, consisting in injecting the same titrant solution ( $\beta$ - or p $\beta$ -CD) in solely the MilliQ<sup>®</sup> water placed in the sample cell, was subtracted from each experimental titration to account for dilution effects.

Data consisting in series of heat flows as a function of time were collected automatically and when appropriate, the interaction process between the two species has been analyzed by the one-site binding model proposed in the Windows-based Origin 7 software package supplied by MicroCal. Based on the concentrations of the titrant and of the sample, the software used a nonlinear least-

squares algorithm (minimization of Chi2) to fit the series of heat flows (enthalpograms) to an equilibrium binding equation, providing best fit values of the stoichiometry (N), association constant ( $K^*$ ) and change in enthalpy ( $\Delta H$ ). From these results, the free energy ( $\Delta G$ ) and the entropy ( $\Delta S$ ) were deducted according to equation 2:

$$\Delta G = -RT \ln K^* = \Delta H - T\Delta S \quad \text{Eq.2}$$

#### 2.2.5. Nanogel Preparation and BZ-3 Loading

- Nanogel suspensions were prepared by mixing MD solution and p $\beta$ -CD solution (polymer concentration (Cp) of 2.5 or 5 g/L) at room temperature under magnetic stirring. The concentrations of both polymer solutions were the same and their respective volumes were varied in order to reach MD/p $\beta$ -CD weight ratio of 33/67, 50/50 or 67/33 w/w.
- BZ-3-loaded nanogels were obtained by mixing the two polymer solutions (MD & p $\beta$ -CD) saturated with BZ-3. The BZ-3-loaded p $\beta$ -CD solutions were prepared as previously described in the solubilization assays section. The required concentrations of MD solutions were prepared by diluting the BZ-3 saturated MD stock solution (50g/L) with a saturated solution of BZ-3 in water.
- BZ-3 loading into MD-p $\beta$ -CD nanogels was evaluated by the calculation of two parameters: (i) the encapsulation efficiency (EE) and (ii) the amount of BZ-3 associated per 100mg of polymer (D).
- The encapsulation efficiency (EE), expressed as a percentage, was calculated according to equation 3:

$$EE (\%) = \frac{L_{BZ-3}}{T_{BZ-3}} \times 100 = \frac{T_{BZ-3} - F_{BZ-3}}{T_{BZ-3}} \times 100 \quad \text{Eq.3}$$

where,  $L_{BZ-3}$  is the loaded BZ-3 (concentration of BZ-3 associated with the nanogels),  $F_{BZ-3}$  the free BZ-3 (concentration of BZ-3 found in the supernatant medium after ultracentrifugation (112,500  $\times$ g, 30 min, 25°C) of the nanogels).  $T_{BZ-3}$  is the total BZ-3 initially brought into the nanogel suspension. All concentrations were expressed in  $\mu\text{g/mL}$ .

(ii) The amount of BZ-3 associated per 100mg of dried polymer was calculated as follows:

$$D \% (w / w) = \frac{L_{BZ-3} (mg)}{P_m (mg)} \times 100 \quad \text{Eq.4}$$

where,  $L_{BZ-3}$  is the amount of BZ-3 effectively entrapped into the nanogel expressed in mg and  $P_m$  the total amount (in mg) of the two polymers, p $\beta$ -CD and MD, that associate to form nanogels.

- The stability of the BZ-3 entrapment over time was investigated by determining the encapsulation efficiency after incubating the suspensions at different temperatures (37 or 4°C) or after subjecting it to temperature cycle between 4 and 25°C.

#### 2.2.6. Yield of Nanogel Production

The yield of nanogel production has been determined to investigate the efficiency of the preparation method. Briefly, 10 mL of nanogel suspension (Cp = 2.5 or 5 g/L; MD/p $\beta$ -CD ratio 50/50 w/w) loaded or non-loaded with BZ-3 was prepared as previously described in section 2.2.5. After 15 min, the suspension was ultracentrifuged (112,500  $\times$ g, 30 min, 25°C). After this step, the samples were composed of a pellet (corresponding to the nanogels) and a supernatant (a water rich phase containing the polymer that did not associate to form the nanogels). Supernatant and pellet were collected separately, freeze-dried and then accurately weighed. The production yield (Eq.5) was calculated from the mass ratio of polymers forming nanogels and total amount of polymer used for the preparation.

$$\text{production yield (\%)} = \frac{\text{amount of polymer in pellet}}{\text{total amount of polymer}} \times 100 \quad \text{Eq. 5}$$

The supernatant containing free polymer have been studied using light scattering techniques. This enabled to assess that there was no signal corresponding to nanogels, as it was the case with nanogel suspension before centrifugation. This evidenced the absence of nanogels in the supernatant.

### 2.2.7. Particle Size Measurement

The hydrodynamic diameter and size distribution of the nanogels were determined at different time intervals by quasi-elastic light scattering (QELS) using a Coulter Nanosizer (Model N4MD, Coultronic, France). If necessary, samples were diluted with MilliQ® water in order to maintain the count per second between  $5 \times 10^4$  and  $1 \times 10^6$ . Each sample was measured three times for 1 min at 20°C and at an angle of 90°. Both unimodal and size distribution processor analysis were performed.

### 2.2.8. Freeze Drying

If necessary, nanogel suspensions were freeze dried. For this purpose, two milliliters of the nanogel suspensions, loaded or non-loaded with BZ-3, were filled in 8 mL glass vials. The samples were frozen at -20°C in a conventional freezer for 24h and then placed into the drying chamber of an alpha I/4 freeze-dryer (Christ, Germany) or a Lyovac GT2 (Leybold-Heraeus), pre-cooled to -20°C. Drying was performed at a pressure of 0.05 mbar for 48 h.

The freeze-dried samples were resuspended by adding 2 mL of MilliQ water under manual shaking for 30 s and the nanogel size was evaluated by QELS as previously described in the size measurements section.

### 2.2.9. Release Studies

For kinetic studies, the freshly prepared nanogel suspension (Cp = 2.5 or 5.0 g/L, MD/pβ-CD = 50/50 w/w) was diluted with water (1 part of NPs with 0.5 part of water) and then placed on a shaker (Heidolph, Titramax 101, Germany) at 37 or 4°C. At each time point (0, 1, 2, 4, 8, 24 and 72h), 1 mL was taken out and ultracentrifuged ( $112,500 \times g$ , 30 min.) to separate the nanogels. The BZ-3 concentration in the supernatant was assessed by UV spectrophotometry as previously described.

In a second study, the effect of dilution of nanogels on the BZ-3 release was investigated at fixed time interval (4 h) and at various temperatures (4 or 37°C). Nanogel suspensions were diluted with increasing volumes of water and after 4h, the amount of BZ-3 released was estimated using the same procedure as described above.

## 3. RESULTS

### 3.1. Solubilization Experiments

The solubilization of BZ-3 by β-CD in its native or polymer form has been investigated using the solubility method described by Higuchi and Connors [33].

- **Determination of the Time Required to Reach the Equilibrium of Complexation**

In a first step, the kinetics of BZ-3 solubilization was determined by adding an excess of the hydrophobic compound into a 10 g/L or a 50 g/L pβ-CD solution. At different time intervals, the concentration of the solubilized BZ-3 was determined. It was found that the BZ-3 concentration reached a plateau value after 8 hours, indicating that the complexation between BZ-3 and pβ-CD reached equilibrium. The same time was required to reach equilibrium in the case of BZ-3/β-CD interaction. Therefore, a longer time of contact between BZ-3 and CDs (monomer or polymer form), i.e. 12 hours, was chosen for the further solubility experiments, to ensure that the experiments were performed under equilibrium state.

- **Phase Solubility Assays**

The equilibrium phase solubility diagrams obtained by using β-CD and pβ-CD are presented in Fig. (2A). As it can be seen from this figure, the BZ-3/β-CD solubility curve was a typical B<sub>S</sub>-type phase solubility diagram [33]. In the first portion of the diagram, the apparent solubility of BZ-3 increased linearly by increasing β-CD concentration up to  $8.8 \times 10^{-3}$  mol/L (10g/L). At higher concentrations, insoluble BZ-3/β-CD complexes were formed. As a consequence, the maximal increase in apparent BZ-3 solubility was  $1 \times 10^{-3}$  mol/L with the addition of β-CD.

Conversely, in the presence of pβ-CD, a continuous linear increase of BZ-3 solubility was observed whatever the β-CD polymer concentration, up to 200 g/L (Fig. 2B). At higher pβ-CD concentrations, the viscosities were too high to carry out the experiments.

At 25°C, the phase solubility diagram was a typical A<sub>L</sub>-type [33] indicating the formation of soluble BZ-3/β-CD complexes for the CD polymer. The apparent stability constant (K<sub>s</sub>) of the BZ-3/β-CD complexes, calculated from the initial straight part of the solubility diagrams (Eq. 1), was  $2260 \text{ M}^{-1}$  for BZ-3/β-CD complexes. For BZ-3/pβ-CD complexes, K was  $5180 \text{ M}^{-1}$ , more than twice as high as found for the BZ-3/β-CD reference sample (Table 1).

The solubilization of BZ-3 by its inclusion into the pβ-CD was also studied at 4 and 37°C (Fig. 2C). The apparent solubility of BZ-3 increased linearly by increasing the pβ-CD concentration for both temperatures studied, as it has been observed at 25°C. The regression curves obtained from the solubility diagrams showed increasing slopes when the temperature rose from 4 to 37°C. At 10 g/L of pβ-CD, the BZ-3 concentration was 1.5-fold higher at 37°C than at 4°C. The apparent stability constants of the complexes formed (calculated using equation 1) were  $10040 \text{ M}^{-1}$  at 4°C and  $4830 \text{ M}^{-1}$  at 37°C.

- **Solubilization of BZ-3 by MD**

Fig. (3) compares the effect of MD, β-CD and pβ-CD on the apparent solubility of BZ-3. As it can be seen, the amount of BZ-3 solubilized increased linearly by increasing the MD concentration, clearly indicating the existence of hydrophobic interactions between the lipophilic BZ-3 and the hydrophobically modified MD polymer.

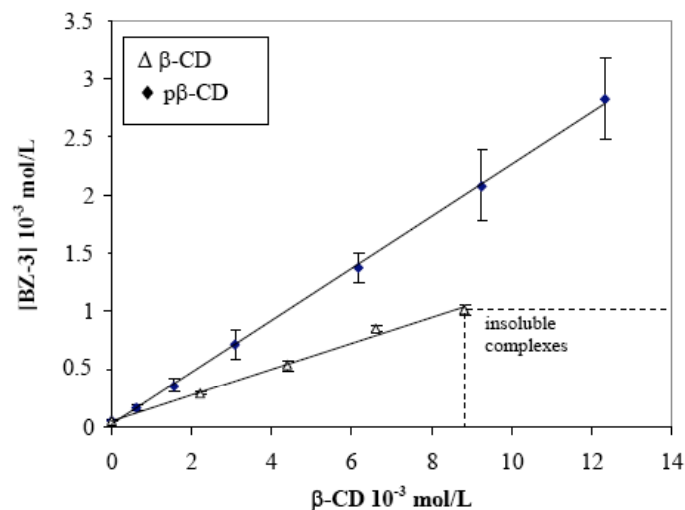
It is noteworthy to point out that the solubilization of BZ-3 was more efficient in the presence of β-CD polymer than in the presence of MD (Fig. 3). Indeed, the concentration of BZ-3 was  $172.7 \pm 15.2$  mg/L in the presence of 5 g/L of pβ-CD (concentration of β-CD cavities in the polymer =  $3.08 \times 10^{-3}$  mol/L) and only  $22.9 \pm 2.9$  mg/L (8-fold lower) in the presence of the same concentration of MD.

### 3.2. Preparation and Characterization of Nanogels Loaded with BZ-3

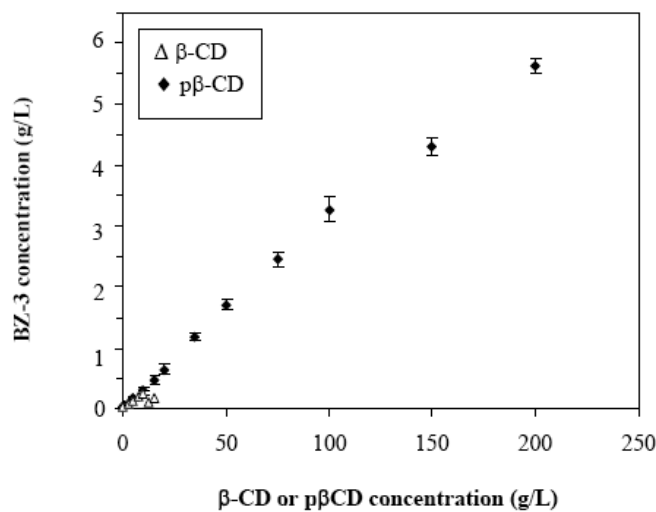
Nanogel suspensions were prepared by mixing MD and pβ-CD solutions at room temperature under magnetic stirring. The characteristics of BZ-3 loaded nanogels obtained by varying polymer concentration and MD/pβ-CD ratio are presented in Table 2.

Nanogels sizing 100 to 200 nm were obtained irrespective of the polymer concentration and the MD/pβ-CD polymer ratio used. Their size distribution was unimodal as indicated by the polydispersity index (PI) value which is less than or equal to 0.2 except in the case of nanogels prepared with a 33/67 w/w MD/pβ-CD polymer ratio (Table 2). The nanogels were freeze-dried and the obtained dried cakes were easily re-hydrated and the suspensions showed mean diameters and PI close to the initial ones measured, i.e. just after nanogel preparation.

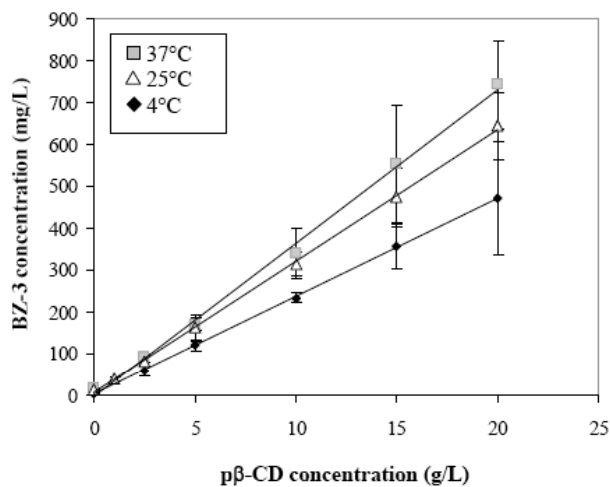
The encapsulation efficiency and the amount of BZ-3 associated per 100mg of dried polymer were highly dependent upon the



A



B



C

**Fig. (2).** Phase solubility diagrams of BZ-3 in the presence of native  $\beta\text{-CD}$  and  $\beta\text{-CD}$  polymer in purified water at 25°C (A)  $\beta\text{-CD}$  molar concentration in the 0 - 14 $\times 10^{-3}$  mol/L range, (B)  $\beta\text{-CD}$  or  $\text{p}\beta\text{CD}$  concentration in the 0 - 200 g/L range. (C) Phase solubility diagrams of BZ-3 in the presence of  $\beta\text{-CD}$  polymer at different temperatures: 4, 25 or 37°C. Each value was the average of three independent experiments  $\pm$  SD.

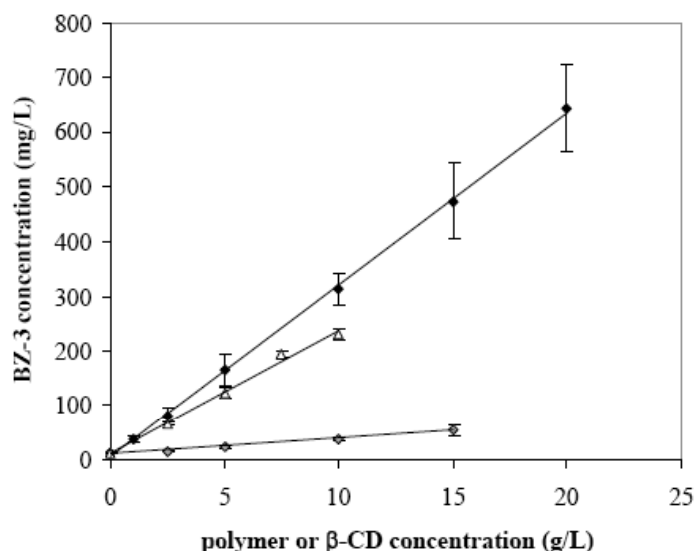


Fig. (3). BZ-3 solubilization in the presence of native  $\beta$ -CD ( $\Delta$ ),  $\beta$ -CD polymer ( $\blacklozenge$ ) and MD polymer ( $\square$ ) in purified water at 25°C. Each value is the average of three independent experiments  $\pm$  SD.

Table 1. Association Constants and Thermodynamic Parameters for Inclusion Complex Formation of BZ-3 (0.0411 mM) with  $\beta$ -CD (10 mM) and p $\beta$ -CD (10 mM) at 298 K (25°C). K and K' are the Association Constants Obtained from the Solubility Curves (Fig. 2A, 2C) and ITC Experiments (Fig. 6), Respectively

CD Derivative	T	K M <sup>-1</sup>	K' M <sup>-1</sup>	$\Delta H$ kJ.mol <sup>-1</sup>	TAS* kJ.mol <sup>-1</sup>	$\Delta G^*$ kJ.mol <sup>-1</sup>
$\beta$ -CD	4°C (277K)	ND	3780	-11.35	7.62	-18.97
	25°C (298K)	2260	2190	-16.69	2.37	-19.06
	37°C (310K)	ND	1460	-33.32	-14.54	-18.78
p $\beta$ -CD	4°C (277K)	10040	3840	-8.14	10.87	-19.01
	25°C (298K)	5180	2700	-17.61	1.96	-19.58
	37°C (310K)	4830	1350	-25.51	-6.93	-18.58

\* $\Delta G = -RT \ln K$ , TAS =  $\Delta H - \Delta G$

\*\*N (N CD : 1 BZ)

ND = not determined

Table 2. Characteristics of BZ-3 Loading into MD/p $\beta$ -CD Nanogels

Cp g/L	MD/p $\beta$ - CD w/w	C <sub>12</sub> / $\beta$ -CD** Molar ratio	C <sub>12</sub> / $\beta$ - CD/BZ3** Molar ratio	EE %	D % (w/w)	Yield of NP formation wt%	Mean Diameter nm / PI	
							Initial*	After Freeze-Drying
2.5	33/67	1/4.7	1/4.7/0.35	31 $\pm$ 5	0.7 $\pm$ 0.1	-	85 $\pm$ 3 / 0.5	105 $\pm$ 37 / 0.6
	50/50	1/2	1/2/0.35	66 $\pm$ 3	1.2 $\pm$ 0.2	83 $\pm$ 2	120 $\pm$ 25 / 0.1	155 $\pm$ 23 / 0.1
	67/33	1/1	1/1/0.2	66 $\pm$ 8	0.9 $\pm$ 0.2	-	135 $\pm$ 20 / 0.1	155 $\pm$ 28 / 0.2
5	33/67	1/4.7	1/4.7/0.6	57 $\pm$ 10	1.2 $\pm$ 0.1	-	100 $\pm$ 24 / 0.4	110 $\pm$ 38 / 0.6
	50/50	1/2	1/2/0.38	75 $\pm$ 5	1.3 $\pm$ 0.1	84 $\pm$ 4	165 $\pm$ 34 / 0.1	120 $\pm$ 23 / 0.2
	67/33	1/1	1/1/0.2	73 $\pm$ 9	0.9 $\pm$ 0.1	-	185 $\pm$ 21 / 0.1	145 $\pm$ 20 / 0.2

Cp: polymer concentration; MD/p $\beta$ -CD: polymer weight ratio; EE: entrapment efficiency; PI: polydispersity index.

D: the amount of BZ-3 associated per 100 mg of dried polymer.

\*Before freeze-drying.

\*\* $\beta$ -CD and C<sub>12</sub> were calculated according to Eqs 6 and 7, respectively.

polymer concentration ( $C_p$ ) and the MD/p $\beta$ -CD ratio. Indeed, the best result was obtained in the case of MD/p $\beta$ -CD ratio of 50/50 w/w irrespective of the  $C_p$ . For instance, in the case of 2.5 g/L nanogels, the drug loading was found to be 1.2 wt% for the 50/50 w/w polymer ratio and only equal to 0.7 and 0.9 wt% for the 33/67 and the 67/33 w/w polymer ratios, respectively.

The yield of nanogel production was determined for the 50/50 w/w polymer ratio using equation 4. It was found that more than 80 % of the polymers associated spontaneously, leading to the formation of nanogels. This value was quite similar to one obtained for non-loaded nanogels ( $80 \pm 3\%$ ), in the case of 2.5 g/L, 50/50 w/w polymer ratio.

The stability of the BZ-3 entrapment was also investigated. For this purpose, BZ-3 loaded nanogels were incubated at two different temperatures: 4°C and 37°C. After predetermined time intervals (0, 1, 2, 4, 8, 24 & 72h), BZ-3 EE was assessed. From the results presented in Fig. (4), in the first two hours, the EE appeared to increase slightly when the suspensions were stored at 4°C whereas the EE slightly decreased when the nanogels were stored at 37°C indicating that BZ-3 entrapment was not significantly affected by the incubation of the nanogels at the temperature of 4 or 37°C.

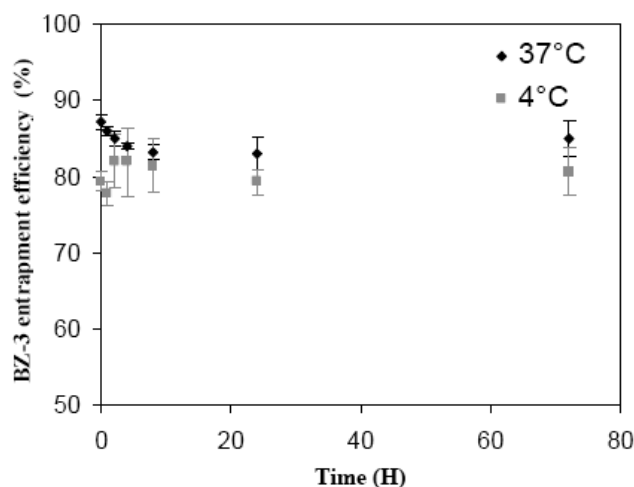


**Fig. (4).** Stability of BZ-3 entrapment into MD/p $\beta$ -CD nanogels during 72 h of incubation at 4 or 37°C. Each value is the average of three independent experiments  $\pm$  SD.

The nanogel suspensions, initially formed at 25°C, were also subjected to successive incubation steps: 2h at 4°C followed by 2h at 25°C. This treatment was then repeated two times. After each incubation step, the BZ-3 loading was calculated. It was found that the initial BZ-3 loading was slightly increased from  $1.44 \pm 0.01$  wt% to  $1.57 \pm 0.02$  wt% after 2h at 4°C. The rise was reversible as demonstrated by the  $1.43 \pm 0.01$  wt% BZ-3 loading reached after 2h storage at 25°C. The same results were obtained up to 5 successive steps of incubation at these temperatures (data not shown).

### 3.3. BZ-3 Release

The kinetics of BZ-3 release was investigated by diluting 1 part of nanogel suspension with 0.5 part of water. The suspensions were incubated at two temperatures (4 and 37°C), and the BZ-3 present in the release medium was assessed at predetermined time intervals. The release kinetics obtained is presented in Fig. (5A). The percentage of BZ-3 released increased in the first 4 hours following nanogel dilution. Then it reached a plateau value around 2.5% and 15% BZ-3 released at 4 and 37°C, respectively.

Therefore, in order to study the influence of nanogel dilution on BZ-3 release, the time of incubation was fixed at 4h and nanogel

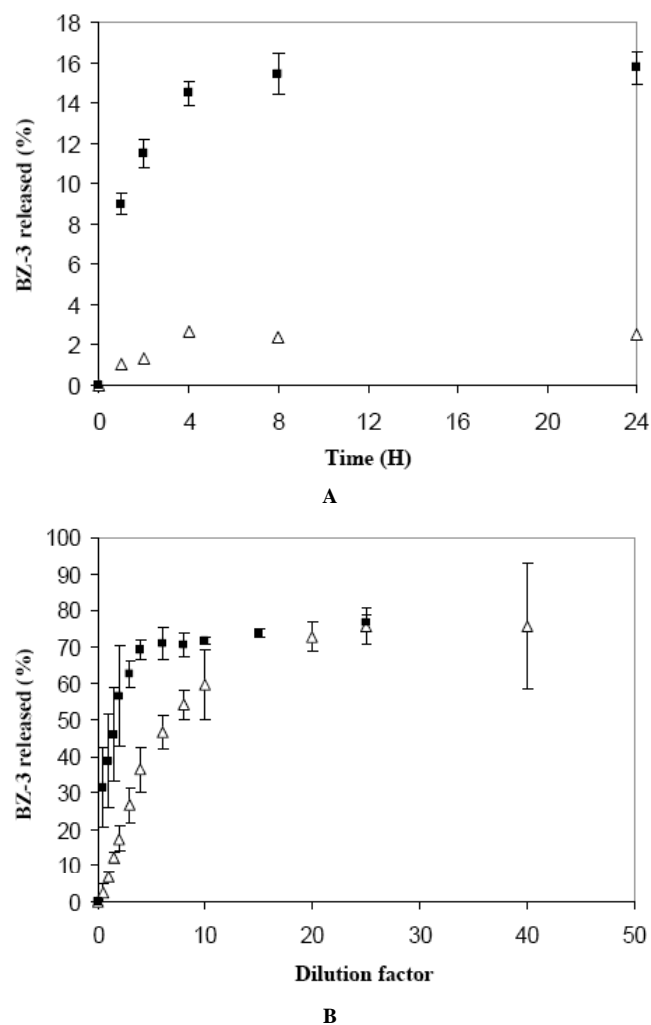


**Fig. (5).** (A) Kinetics of BZ-3 release at 4 ( $\Delta$ ) or 37°C ( $\blacksquare$ ). Nanogels were diluted with water immediately after their preparation. At predetermined time intervals, the amount of BZ-3 was assessed in the release medium. (B) Effect of nanogels dilution on the BZ-3 release at 4 ( $\Delta$ ) or 37°C ( $\blacksquare$ ). Nanogel suspensions were diluted with increasing volumes of water, 4h after dilution the amount of BZ-3 was assessed in the release medium. Each value is the average of three independent experiments  $\pm$  SD.

suspensions were diluted with increasing the amounts of water, and placed at 4 or 37°C. Then the percentage of BZ-3 present in the release medium was determined and plotted against the dilution factor (Fig. 5B). The first observation was that the percentage of BZ-3 released increased by increasing the dilution of the nanogels suspension. For example, at 37°C the percentage of BZ-3 released increased from 30% to 70% when the dilution factor increased from 1 to 5. When the dilution factor became higher than 5, the amount of BZ-3 released was increased slightly.

The second observation was that the release was less important at 4°C than at 37°C. Indeed, 70% of BZ-3 was released for a dilution factor of 5 at 37°C versus only 35% for the same dilution at 4°C. Moreover, the equilibrium (70% of BZ-3 released) was reached at a dilution factor of 20 at 4°C while the maximum BZ-3 released was obtained for a dilution factor of 5 at 37°C.

### 3.4. Isothermal Titration Microcalorimetry

The thermodynamics of the interaction between BZ-3 and  $\beta$ -CD in its monomer or polymerized form has been investigated using ITC at three different temperatures (4, 25 and 37°C). Typical ITC

data corresponding to the binding interaction of BZ-3 and  $\beta$ -CD in its native form or polymerized form are presented in Fig. (6). The integration of the exothermic heat flows which were released upon successive injection of 10  $\mu$ L aliquots of CDs into BZ-3 solution leads to a differential binding curve which was fitted to a standard single-site binding model leading to the direct determination of  $N$ ,  $K'$  and  $\Delta H$  changes of the interaction. The association constants and the thermodynamic parameters of the association between BZ-3 and  $\beta$ -CD or  $p\beta$ -CD at different temperatures are presented in Table 1.

The first observation was that at a given temperature, the association constants  $K'$  were in the same order of magnitude for BZ-3/ $\beta$ -CD and BZ-3/ $p\beta$ -CD complexes. For instance, at 25°C  $K'$  of BZ-3/ $\beta$ -CD and BZ-3/ $p\beta$ -CD interactions were found equal to 2190  $M^{-1}$  and 2700  $M^{-1}$  respectively. The second observation was that when the temperature of the experiment was increased from 4°C to 37°C,  $K'$  decreased. For example,  $K'$  of BZ-3/ $p\beta$ -CD interaction decreased from 3840  $M^{-1}$  at 4°C to 1350  $M^{-1}$  at 37°C. The stoichiometries ( $N$ ) of the complexes formed were found consistent with a 1:1 stoichiometry for both BZ-3/ $\beta$ -CD and BZ-3/ $p\beta$ -CD interactions (Fig. 6, right panels).

From a thermodynamic point of view, both BZ-3/ $\beta$ -CD and BZ-3/ $p\beta$ -CD interactions were characterized by a negative  $\Delta H$  value and a positive  $T\Delta S$  value except in the case of inclusion complexes formed at 37°C, for which  $T\Delta S$  took a negative value (Table 1).

Moreover,  $\Delta H$  and  $T\Delta S$  decreased when the temperature increased, always leading to a negative  $\Delta G$  value of about  $-19 \text{ kJ}\cdot\text{mol}^{-1}$ .

## 4. DISCUSSION

### 4.1. BZ-3 Solubilization

#### Using $\beta$ -CD and $p\beta$ -CD

The formation of BZ-3/CD inclusion complexes resulted in an increase in the apparent water solubility of the sparingly soluble sunscreen agent. The results obtained clearly demonstrate the advantage of using  $p\beta$ -CD polymers instead of the native  $\beta$ -CD to improve the apparent solubility of BZ-3 (Fig. 2). Indeed, the solubilization of the hydrophobic molecule was limited by the poor solubility of  $\beta$ -CD in water [34] (18.5 g/L equivalent to  $1.6 \times 10^{-2} \text{ mol/L}$ ). Thus, the inclusion complexes formed were also poorly soluble in water. Conversely, the highly water-soluble  $p\beta$ -CD polymer allowed a spectacular increase of the hydrophobic molecules' solubility. For example, the apparent solubility of BZ-3 was increased by a factor of 50 in the presence of 10g/L  $\beta$ -CD and a factor of 90 and 1500 in the presence of 10 g/L and of 200 g/L  $p\beta$ -CD, respectively (Fig. 2B).

The stability constants have been assessed from the solubility isotherms (Fig. 2) obtained by plotting the concentration of BZ-3 against the concentration of CD, with the assumption that the complexes formed had a 1:1 stoichiometry (Eq.1). The 1:1 stoichiome-

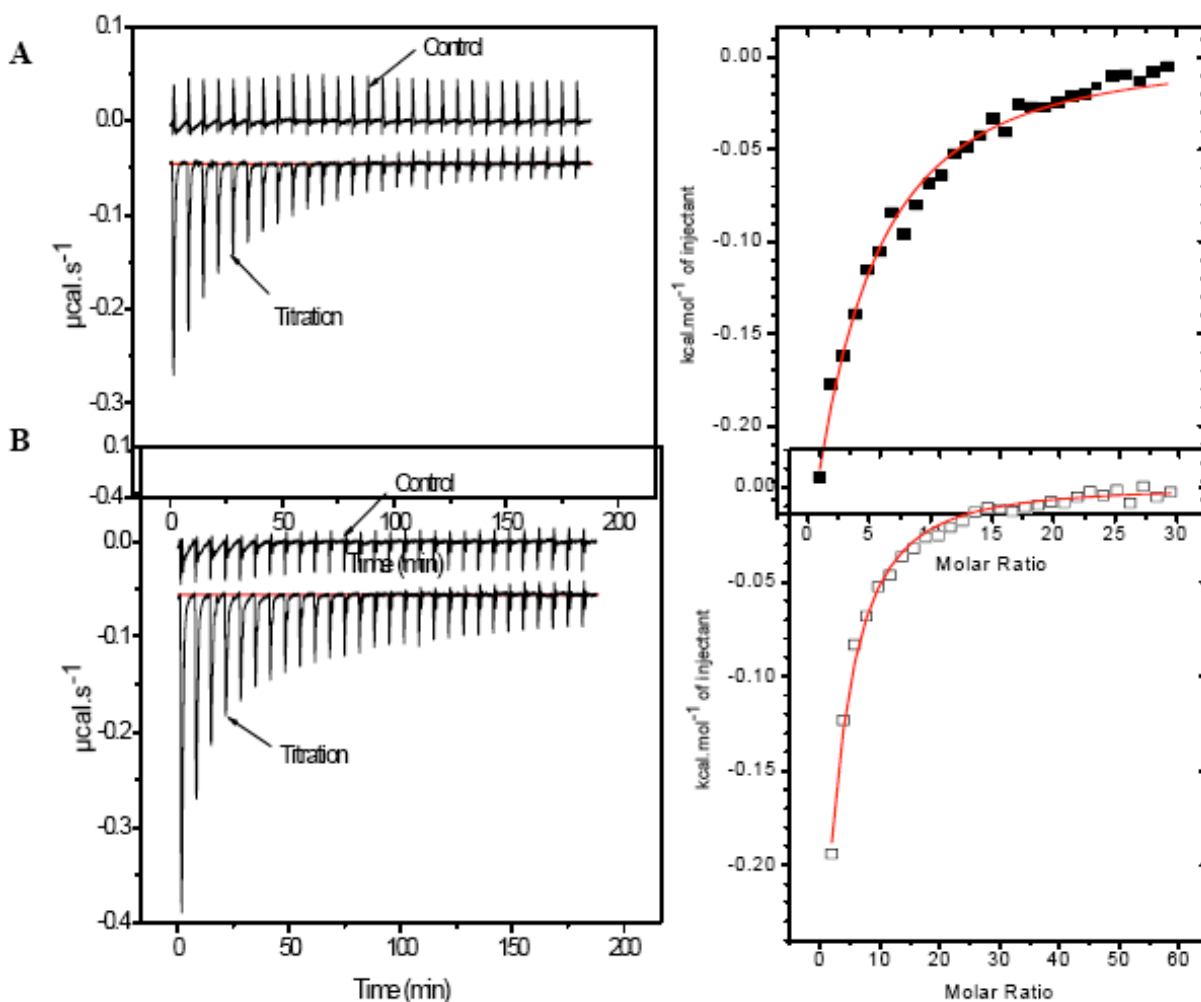


**Fig. (6).** Typical ITC data corresponding to the binding interaction of BZ-3 (0.0411 mM, 1.441 ml cell volume) with (A)  $\beta$ -CD (10 mM) ( $\blacksquare$ ) and (B)  $p\beta$ -CD (10 mM) ( $\square$ ) at 4°C. Left panels show exothermic heat flows which are released upon successive injection of 10  $\mu$ L aliquots of cyclodextrin into BZ-3. The right panels show integrated heat data, giving a differential binding curve which was fit to a standard single-site binding model yielding the following parameters  $N$ ,  $K'$ , and  $\Delta H$ .

try of the interaction was confirmed by using ITC (Fig. 6). However, it is noteworthy to point out that, in the case of BZ-3/p $\beta$ -CD, the association constant values obtained from ITC experiments were not in accordance with the ones obtained from phase solubility studies. Indeed, at 25°C the BZ-3/p $\beta$ -CD association constants were equal to 5180 M<sup>-1</sup> and 2700 M<sup>-1</sup> when obtained from solubility studies and ITC experiments, respectively (Table 1).

Despite the fact that phase-solubility diagrams are the most common method for the determination of the association constants, this techniques has been recently questioned mainly by Loftsson [35] who pointed out that association constants might be overestimated by this way. Indeed, the apparent association constants obtained from phase-solubility diagrams reflects drug solubilisation by many possible mechanisms other than simple inclusion inside the CD cavities. Thus, several research groups have shown that CDs form both inclusion and non-inclusion complexes and that many different types of complexes can coexist in aqueous solutions [36, 37]. In addition, both CDs and CD complexes are known to form aggregates and it is thought that these aggregates are able to solubilize drugs and other hydrophobic molecules through micellar-type mechanisms [35, 38]. Furthermore, in the case of CD polymers, the situation is more complex than for CD monomers, because the glyceryl linkers between the CDs might act as solubilizers for hydrophobic molecules [37]. Thus, in the p $\beta$ -CD polymer obtained by crosslinking with epichlorohydrin, the hydrophobic pyrene molecules fit well inside the clam shells arrangements between two  $\beta$ -CDs. This might be the case with our BZ-3/p $\beta$ -CD system, where BZ-3 molecules might also accumulate inside hydrophobic non-inclusion pockets in p $\beta$ -CD, until their saturation. Contrarily, the saturation of these pockets could not occur in the case of ITC experiments, because BZ-3 is already in its molecular form in the measurement cell. As a consequence, association constants determined from phase-solubility diagrams appear to be overestimated.

So far in the present study, ITC represented the most accurate method for the evaluation of the association constant related to the complexation of BZ-3 with both  $\beta$ -CD and p $\beta$ -CD. Indeed, the superiority of ITC over all other methodologies is the possibility to get deep understanding of the molecular interaction between BZ-3 and CDs through the determination of the association constant and thermodynamic parameters. This determination is independent on the solubilization of the drug since both BZ-3 and CD are in their soluble form.

An interesting observation is that *K* was strongly affected by the temperature of the experiment. Indeed, both ITC and solubility experiments have shown that *K* decreased when the temperature increased from 4°C to 37°C (Table 1). The dependence of the association constant upon temperature is a well known phenomenon and has been widely described in CD literature. For instance, Todorova *et al.* have shown that in the case of inclusion of three drugs naproxen, flurbiprofen and nabumetone into  $\beta$ -CD and  $\gamma$ -CDs, the association constants decreased with the temperature [39]. Similar results have been reported for the inclusion of naproxen and ketoprofen into modified  $\beta$ -CDs inclusion complexes [40, 41].

#### Using MD

The apparent solubility of BZ-3 was also improved in the presence of MD polymer (Fig. 3) but to a much lower extent than with CDs. The enhancement of BZ-3 solubility using MD may result from interactions between the poorly soluble BZ-3 and the microdomains formed upon the assembly of the hydrophobic alkyl-chains grafted onto the hydrophilic dextran backbone. Indeed, precedent work has demonstrated that these hydrophobic side groups led to the formation of polymeric micelles [42]. The critical aggregation concentration (CAC) of MD (in the same range of substitution yield as here), which corresponded to the onset of the formation of hydrophobic microdomains, was about 0.2 g/L, as determined by surface tension measurements [20]. The present study was carried

out at higher MD concentration, where the hydrophobic dodecyl moieties of MD associate as micelles. Therefore, the observed increase in BZ-3 solubilities could be reasonably attributed to their solubilization into the hydrophobic microdomains of the amphiphilic MD.

#### 4.2. Characterization of BZ-3 Loading into Nanogels

We further took advantage of the ability of BZ-3 to complex with p $\beta$ -CD and to interact with MD, to entrap it into the associative MD/p $\beta$ -CD nanogels. On the basis of previous results showing a short physical stability of MD/p $\beta$ -CD nanoassemblies at polymer concentrations (*C<sub>p</sub>*) higher than 5 g/L [43], the nanogels were prepared using *C<sub>p</sub>* of 2.5 g/L and 5 g/L and three polymer weight ratios: 33/67, 50/50 and 67/33 (w/w). For BZ-3 entrapment, it was chosen to form nanogels by mixing p $\beta$ -CD and MD solutions, already loaded with BZ-3. In both polymer solutions, the hydrophobic molecule was solubilized at saturation. Therefore, it was expected that the dissociation of CD/BZ-3 complexes upon dilution (arising from solution mixing) would be limited. The results obtained have demonstrated that the polymer ratio had an impact on the nanogel formation as well as on the entrapment of BZ-3. Indeed, in all the conditions tested nanogels of 100-200 nm with unimodal distribution were obtained, except for the 33/67 (w/w) ratio (Table 2). Moreover, nanogels formed with a 50/50 (w/w) polymer ratio exhibited the highest BZ-3 entrapment (drug loading of 1.3 wt%).

Though the results of phase solubility and ITC experiments confirmed the formation of 1:1 stoichiometry of BZ-3: $\beta$ -CD, the achieved drug loading was about 1.3 wt%. This could be attributed to the fact that not all the CDs in the  $\beta$ -CD polymer can form inclusion complexes. Indeed, there is equilibrium between BZ-3 in the complexed form and BZ-3 free in solution. Moreover, it is possible that steric effects due to crosslinking of  $\beta$ -CD in the p $\beta$ -CD polymers might prevent part of the CDs to act like hosts for BZ-3.

As the formation of nanogels is based on the association of MD and p $\beta$ -CD through the complexation between alkyl moieties (*C<sub>12</sub>*) and CD cavities, it was a key point to determine the molar ratio *C<sub>12</sub>*/ $\beta$ -CD for each MD/p $\beta$ -CD weight ratio used for nanogel preparation.

The molar ratio *C<sub>12</sub>*/ $\beta$ -CD/BZ-3 for each MD/p $\beta$ -CD weight ratio used for nanogel preparation was calculated from the molar number of  $\beta$ -CD cavities, lauryl chains and BZ-3 molecule given by Eqs. 6, 7 and 8 respectively:

$$\text{Number of } \beta\text{-CD cavities (molar)} = \frac{m_{p\beta\text{CD}} \cdot 0.7}{M_{\beta\text{CD}}} \quad \text{Eq.6}$$

where, *m<sub>p $\beta$ -CD</sub>*

 is the mass of p $\beta$ -CD used in the experiment, 0.7 is the  $\beta$ -CD content in the polymer and *M* is the molecular weight of a  $\beta$ -CD.

$$\text{Number of } C_{12} \text{ chains} = \frac{m_{MD} \cdot \tau}{M_D} \quad \text{Eq.7}$$

where, *m<sub>MD</sub>* is the mass of MD used in the experiment,  $\tau$  is the molar percentage of glucose units bearing *C<sub>12</sub>* moieties in the polymer (4.8%) and *M<sub>D</sub>* is the molecular weight of one glucose units.

$$\text{Number of BZ-3 (molar)} = \frac{m_{BZ-3}}{M_{BZ-3}} \quad \text{Eq.8}$$

Where, *m<sub>BZ-3</sub>* is the mass of BZ-3 used in the experiment and *M<sub>BZ-3</sub>* is the molecular weight of the BZ-3 molecule.

By performing these calculations, the 50/50 (w/w) ratio was found to correspond to 1*C<sub>12</sub>*/2 $\beta$ -CD. At this molar ratio, 80% of the polymers in the formulation associated to form nanogels loaded or non-loaded with BZ-3, indicating that the presence of the hydro-

phobic alkyl-chains did not impede with the polymer association through C<sub>12</sub>/β-CD complexation.

Despite the occupancy of β-CD cavities by BZ-3 molecules, enough CDs remained available to complex the C<sub>12</sub> chains of MD polymer. Moreover, as BZ-3 entrapment was maximum, it can be concluded that 1C<sub>12</sub>/2CD molar ratio was the optimum for the formation of BZ-3 loaded nanogels. The lower entrapment obtained for other polymer weight ratios, suggests a less efficient polymer association. The 33/67 MD/pβ-CD weight ratio corresponded to molar ratio of 1C<sub>12</sub>/5β-CD, showing an excess of β-CD regarding to alkyl chains. Therefore, one could suppose that not enough C<sub>12</sub>/CD complexes were formed to permit the formation of nano-assemblies (nanogels) of sufficient cohesion when the two polymers were associated. Probably, in the nanogel samples, nanoassemblies coexist with non-associated polymer particles of pβ-CD, thus explaining the high polydispersity of the samples (Table 2). The 67/33 (w/w) ratio corresponded to a 1C<sub>12</sub>:1β-CD molar ratio. Due to the compact conformation of the branched β-CD polymer in water [44], some CDs were probably masked, unavailable for C<sub>12</sub> chains complexation. Moreover, some CD cavities in the pβCD polymer were complexed with BZ-3. Therefore, the number of C<sub>12</sub>/CD inclusion complexes formed was also insufficient for efficient polymer association.

Depending on the sun protection factor to be achieved, UV filters such as BZ-3 are added up to maximal concentrations of 6% (US) 10% (Australia, Europe) and 5% (Japan). However, since the first effective sunscreen developed in about 60 years ago, a main concern nowadays is the damage on the skin resulting from some sunscreen chemicals which produce potentially harmful substances if they are illuminated while in contact with living cells [45].

The amount of sunscreen which penetrates through the stratum corneum may or may not be large enough to cause damage. Recently, the amount of harmful reactive oxygen species (ROS) reflecting skin damage was measured in untreated and in sunscreen-treated skin [46]. In the first 20 minutes the film of sunscreen had a protective effect and the number of ROS species was low. After 60 minutes, however, the amount of absorbed sunscreen was so high that the amount of ROS increased more in the sunscreen-treated skin than in the untreated skin [46].

Thus, the benefits that might result from a formulation that retain BZ-3 on the skin are invaluable, given the frequency of application of sunscreens. Nanoparticulate systems are supposed not to cross the skin barrier because of their large size. Lower BZ-3 concentrations in such nanoparticle or nanogel-based formulations could be envisageable, if indeed BZ-3 would not penetrate through the skin causing damages. However, many other investigations would be necessary to confirm these assumptions and for the further development of our system.

#### 4.3. Stability of BZ-3 Entrapment and Release

The stability of BZ-3 entrapment was studied for the optimized loaded nanogels (C<sub>p</sub>= 2.5 or 5 g/L, MD/pβ-CD=50/50 w/w) by incubating the nanogels at 4°C or 37°C. Slight changes in BZ-3 entrapment were observed during the first hours of incubation. Entrapment slightly decreased at 37°C and slightly increased at 4°C, indicating a moderate effect of the temperature (Fig. 4). Moreover, the changes in BZ-3 entrapment with respect to changes in temperature were reversible as evidenced by subjecting the samples to successive steps where temperature decreased from 25 to 4°C and then increased in the same range. These modifications were expected as it was previously found that the association constants of BZ-3/CD increased when the temperature decreased.

The entrapped BZ-3 was released upon nanogel dilution. Kinetic studies have evidenced that the amount of released BZ-3 increased in the first four hours (Fig. 5A). Then, the release reached equilibrium and a new dilution was required to allow additional

BZ-3 release. The percentage of sunscreen released rose with increasing dilutions leading to a maximal release of 70% (Fig. 5B). Thus, a significant part of BZ-3 remained firmly associated to the nanogels. Size measurements have been performed for each dilution made: the nanogels conserved the same mean diameter with unimodal distribution. These findings suggest that nanogels did not dissociate upon dilution.

As expected, BZ-3 release was influenced by temperature. Indeed, due to lower association constants of BZ-3/CD complexes at 37°C than at 4°C, the percentage of BZ-3 released was higher at 37°C than at 4°C, for the same dilution. As a consequence, a 2.5-fold higher dilution was needed at 4°C than at 37°C to reach the maximum BZ-3 release of 70%. As the dilution phenomena are limited at the skin surface, one could expect that the sunscreen agent would remain well entrapped into the nanogels after skin application. Further experimentations will be carried out *in vitro* to evidence the efficiency of BZ-3 entrapment into the associative MD/pβ-CD nanogels to prevent skin penetration.

#### 4.4. Storage of the Nanogels

Storage of BZ-3 nanogels as suspensions might presents some drawbacks such as the risk of microbiological contamination, the premature polymer degradation by hydrolysis and physicochemical instability. Thus, it has been shown previously that destabilization of MD/pβ-CD nanogels could be circumvented by their storage after freeze-drying [43]. In this study, we showed that BZ-3 loaded nanogels could be easily reconstituted after freeze drying with mean diameters comparable with the initial ones (Table 2).

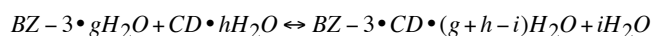
#### 4.5. Thermodynamic Parameters

Upon the interaction of BZ-3 with CD cavity, a balanced enthalpic and entropic variation could reflect many events including desolvation of water molecules bound to the BZ-3 and/or to the CD and formation of weak interactions. Among the several possible weak interactions involved in the complexation of guests with CDs, van der Waals forces and hydrophobic interactions related to the size/shape matching between the guest and the CD cavity have been reported [15, 16, 22, 32, 47]. An acute analysis of the thermodynamic parameters ( $\Delta H$ ,  $\Delta S$ ) could allow evidencing the main driving forces involved in the complexation process. Typically, hydrophobic interactions between two apolar molecules at room temperature have been described as entropy-driven processes, where the entropy of the interaction is large and positive while the enthalpy of the process is small ( $|\Delta H| < |T\Delta S|$ ) [15, 16, 32, 48]. However, van der Waals interactions are usually enthalpy-driven processes with minor favourable or unfavourable entropies of interaction ( $|\Delta H| > |T\Delta S|$ ) [22].

It can be seen from Table 1, both  $\Delta H$  and  $\Delta S$  variations were clearly affected by the temperature of the experiment, being either favorable or unfavorable. Indeed, at 25°C and 37°C, the reactions of complexation of BZ-3 with both β- and pβ-CD were exclusively exothermic phenomena ( $\Delta H < 0$ ) with favorable entropic contribution ( $\Delta S > 0$ ) and mostly enthalpy driven ( $|\Delta H| > |T\Delta S|$ ). Thus, it can be concluded that the main driving forces of the binding at 25 and 37°C are van der Waals forces [22].

However, at 4°C, the interaction of BZ-3 with both β-CD and pβ-CD resulted in an increase of the  $\Delta S$  (7.62 and 10.87 kJ.mol<sup>-1</sup> for β-CD and pβ-CD respectively). The large gain in  $\Delta S$  could be attributed to the strongest interaction between BZ-3 and CD cavity resulting in a more pronounced desolvation. Noteworthy, desolvation occurs: *i*) upon BZ-3 inclusion in CDs and *ii*) from dehydration of the peripheral hydroxyl groups in the bridges between CDs, upon the formation of non-inclusional complexes in pβ-CD.

Taking into account the initially included or interacting water molecules, the 1:1 complexation interaction of BZ-3 with a CD host may be written as follows:



Eq.9

Where  $g$  represents the number of water molecules interacting with the free BZ-3,  $h$  the number of tightly bound hydration water molecules inside the free CD cavity, and  $i$  the net displacement of water upon complexation.

The desolvation process and, in turn, the entropic gain were more pronounced in the case of p $\beta$ -CD. One possible explanation for this increased entropy contribution could be related to the more hydrophilic environment of the CD cavity in the p $\beta$ -CD polymer: the reorganization of surface/cavity neighbouring water molecules that were released upon BZ-3 inclusion could be higher in the case of p $\beta$ -CD polymer than in native  $\beta$ -CD [31]. From these findings, it could be concluded that the interactions between BZ and cyclodextrins represented the net effect of solvation changes (hydrophobic hydration) and van der Waals interactions with the predominance of each type of forces when the temperature of the experiment was changed.

The changes in enthalpy were compensated by the changes in entropy always leading to a negative  $\Delta G$  value of about  $-19 \text{ kJ} \cdot \text{mol}^{-1}$ . A good straight line ( $R^2=0.997$ ) could be obtained when plotting  $\Delta H$  versus  $T\Delta S$  for the different reactions of complexation of BZ-3 with  $\beta$ -CD and p $\beta$ -CD. This confirmed the existence of an enthalpy-entropy compensation effect (Fig. 7).

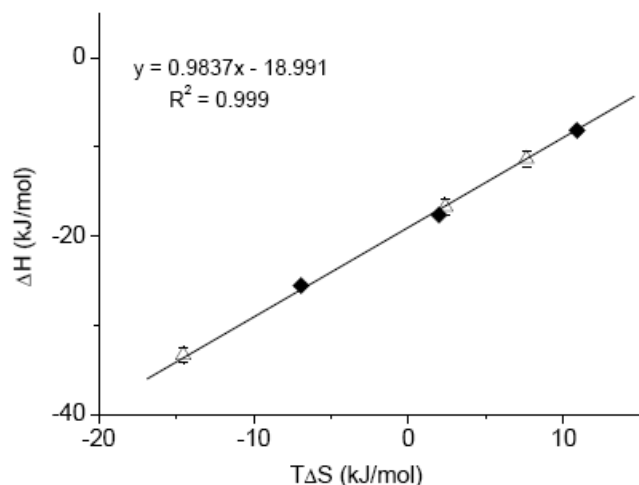


**Fig. (7).** Enthalpy-entropy compensation plot corresponding to inclusion complex formation of BZ-3 (0.025mM) with  $\beta$ -CD (10mM) (◇) and p $\beta$ -CD (10mM) (◆). Temperature of the experiment was changed (4, 25 and 37°C). See Table 1 for the original data.

## 5. CONCLUSION

The solubility of BZ-3 was remarkably increased by host-guest interactions between  $\beta$ -CD cavities of p $\beta$ -CD and hydrophobic BZ-3. Monodisperse BZ-3 loaded nanogels were prepared by a one-step method based on the mixing of two water soluble self-assembling polymers. Very high BZ-3 entrapment and nanogel production yields were obtained. The BZ-3 release increased with increasing dilutions, indicating that dilution of nanogels is a prerequisite for the release, which makes the system interesting for sunscreen formulation to prevent systemic penetration of BZ-3. Attractive features of these self-assembling systems are their 'green' (solvent free) preparation method, small size and the ease of redispersion without altering the size after freeze drying.

## REFERENCES

- [1] Gonzalez, H.; Farbrot, A.; Larko, O.; Wennberg, A.M. Percutaneous absorption of the sunscreen benzophenone-3 after repeated whole-body

applications, with and without ultraviolet irradiation. *Br. J. Dermatol.*, **2006**, *154*, 337-340.

- [2] Rastogi, S.C. UV filters in sunscreen products - a survey. *Contact Derm.*, **2002**, *46*, 348-351.
- [3] National Library of Medicine. Household Products Database. <http://hpd.nlm.nih.gov/cgi-bin/household/brands?tbl=chem&id=326&query=Benzophenone-3&searchas=TblChemicals> (Accessed August 30, 2010)
- [4] Hayden, C.G.; Roberts, M.S.; Benson, H.A. Systemic absorption of sunscreen after topical application. *Lancet*, **1997**, *350*, 863-864.
- [5] Hayden, C.G.; Cross, S.E.; Anderson, C.; Saunders, N.A.; Roberts, M.S. Sunscreen penetration of human skin and related keratinocyte toxicity after topical application. *Skin Pharmacol. Physiol.*, **2005**, *18*, 170-174.
- [6] Janjua, N.R.; Mogensen, B.; Andersson, A.M.; Petersen, J.H.; Henriksen, M.; Skakkebaek, N.E.; Wulf, H.C. Systemic absorption of the sunscreens benzophenone-3, octyl-methoxycinnamate, and 3-(4-methyl-benzylidene) camphor after whole-body topical application and reproductive hormone levels in humans. *J. Invest. Dermatol.*, **2004**, *123*, 57-61.
- [7] Treffel, P.; Gabard, B. Skin penetration and sun protection factor of ultraviolet filters from two vehicles. *Pharm. Res.*, **1996**, *13*, 770-774.
- [8] Sarveiya, V.; Risk, S.; Benson, H.A.E. Liquid chromatographic assay for common sunscreen agents: application to *in vivo* assessment of skin penetration and systemic absorption in human volunteers. *J. Chromatogr. B Anal. Technol. Biomed. Life Sci.*, **2004**, *803*, 225-231.
- [9] Schmidt, T.; Ring, J.; Abeck, D. Photoallergic contact dermatitis due to combined UVB (4-methylbenzylidene camphor/octyl methoxycinnamate) and UVA (benzophenone-3/butyl methoxydibenzoylmethane) absorber sensitization. *Dermatology*, **1998**, *196*, 354-357.
- [10] Wolf, P.; Donawho, C.K.; Kripke, M.L. Effect of sunscreens on UV radiation-induced enhancement of melanoma growth in mice. *J. Natl. Cancer Institute*, **1994**, *86*, 99-105.
- [11] Schlumpf, M.; Cotton, B.; Conscience, M.; Haller, V.; Steinmann, B.; Lichtensteiger, W. *In vitro* and *in vivo* estrogenicity of UV screens. *Environ. Health Perspect.*, **2001**, *109*, 239-244.
- [12] Schlumpf, M.; Schmid, P.; Durrer, S.; Conscience, K. Endocrine activity and developmental toxicity of cosmetic UV filters-an update. *Toxicology*, **2004**, *205*, 113-122.
- [13] Jiang, R.; Benson, H.A.E.; Cross, S.E.; Roberts, M.S. *In vitro* human epidermal and polyethylene membrane penetration and retention of the sunscreen benzophenone-3 from a range of solvents. *Pharm. Res.*, **1998**, *15*, 1863-1868.
- [14] Uekama, K.; Hirayama, F. In: *The Practice of Medicinal Chemistry*; Wermuth, C.G., Ed.; Academic Press: UK, **2003**; pp 649-673.
- [15] Loftsson, T.; Brewster, M.E. Pharmaceutical applications of cyclodextrins. 1. Drug solubilization and stabilization. *J. Pharm. Sci.*, **1996**, *85*, 1017-1025.
- [16] Brewster, M.E.; Loftsson, T. Cyclodextrins as pharmaceutical solubilizers. *Adv. Drug Deliv. Rev.*, **2007**, *59*, 645-666.
- [17] Segura-Sanchez, F.; Bouchemal, K.; Lebas, G.; Vauthier, C.; Santos-Magalhaes, N.S.; Ponchel, G. Elucidation of the complexation mechanism between (+)-usnic acid and cyclodextrins studied by isothermal titration calorimetry and phase-solubility diagram experiments. *J. Macromol. Recog.*, **2009**, *22*, 232-241.
- [18] Duchêne, D.; Glomot, F.; Vaution, C. In: *Cyclodextrins and their industrial uses*; Duchêne, D., Ed.; Editions de Santé: Paris, **1987**; pp 211-257.
- [19] Uekama, K.; Otogiri, M. Cyclodextrins in drug carrier systems. *Crit. Rev. Ther. Drug Carrier Syst.*, **1987**, *3*, 1-40.
- [20] Gref, R.; Amiel, C.; Molinard, K.; Daoud-Mahammed, S.; Sebille, B.; Gillet, B.; Beloeil, J.C.; Ringard, C.; Rosilio, V.; Poupaert, J.; Couvreur, P. New self-assembled nanogels based on host-guest interactions: characterization and drug loading. *J. Control Release*, **2006**, *111*, 316-24.
- [21] Rekharsky, M.V.; Inoue, Y. In: *Cyclodextrins and Their Complexes*; Dodziuk, H., Ed.; Wiley-VCH Verlag GmbH & Co KGaA: Weinheim, **2006**; pp 199-230.
- [22] Inoue, Y.; Hakushi, T.; Tong, L.; Shen, B.; Jin, D. Thermodynamics of molecular recognition by cyclodextrins. 1. Calorimetric titration of inclusion complexation of naphthalenesulfonates with  $\alpha$ -,  $\beta$ -, and  $\gamma$ -cyclodextrins: enthalpy-entropy compensation. *J. Am. Chem. Soc.*, **1993**, *115*, 475-481.
- [23] Bouchemal, K. New challenges for pharmaceutical formulations and drug delivery system characterisation using isothermal titration calorimetry. *Drug Discov. Today*, **2008**, *13*, 960-972.
- [24] Othman, M.; Bouchemal, K.; Couvreur, P.; Gref, R. Microcalorimetric investigation on the formation of supramolecular nanoassemblies of associative polymers loaded with gadolinium chelate derivatives. *Int. J. Pharm.*, **2009**, *379*, 218-225.

- [25] Tong, W.Q.; Lach, J.L.; Chin, T.F.; Guillory, K. Microcalorimetric investigation of the complexation between 2-hydroxypropyl-beta-cyclodextrin and amine drugs with the diphenylmethyl functionality. *J. Pharm. Biomed. Anal.*, **1991**, *9*, 1139-1146.
- [26] De Sousa, F.B.; Denadai, A.M.L.; Lula, I.S.; Lopes, J.F.; Dos Santos, H.F.; De Almeida, W.B.; Sinisterra, R.D. Supramolecular complex of fluoxetine with  $\beta$ -cyclodextrin: An experimental and theoretical study. *Int. J. Pharm.*, **2008**, *353*, 160-169.
- [27] Denadai, A.M.L.; Teixeira, K.I.; Santoro, M.M.; Pimenta, A.M.C.; Cortes, M.E.; Sinisterra, R.D. Supramolecular self-assembly of  $\beta$ -cyclodextrin: an effective carrier of the antimicrobial agent chlorhexidine. *Carbohydr. Res.*, **2007**, *342*, 2286-2296.
- [28] Charlot, A.; Heyraud, A.; Guenot, P.; Rinaudo, M.; Auzély-Velty, R. Controlled synthesis and inclusion ability of a hyaluronic acid derivative bearing  $\beta$ -cyclodextrin molecules. *Biomacromol.*, **2006**, *7*, 907-913.
- [29] Gomez, C.G.; Chambat, G.; Heyraud, A.; Villar, M.; Auzély-Velty, R. Synthesis and characterization of a  $\beta$ -CD-alginate conjugate. *Polymer*, **2006**, *47*, 8509-8516.
- [30] Ollila, F.; Pentikäinen, O.T.; Forss, S.; Johnson, M.; Slotte, J.P. Characterization of bile salt/cyclodextrin interactions using isothermal titration calorimetry. *Langmuir*, **2001**, *17*, 7107-7111.
- [31] Daoud-Mahammed, S.; Couvreur, P.; Bouchemal, K.; Cheron, M.; Lebas, G.; Amiel, C.; Gref, R. Cyclodextrin and polysaccharide-based nanogels: entrapment of two hydrophobic molecules, benzophenone and tamoxifen. *Biomacromolecules*, **2009**, *10*, 547-554.
- [32] Rekharsky, M.V.; Inoue, Y. Complexation thermodynamics of cyclodextrins. *Chem. Rev.*, **1998**, *98*, 1875-1917.
- [33] Higuchi, T.; Connors, K.A. Phase solubility techniques. *Adv. Anal. Chem. Instrum.*, **1965**, *4*, 117-212.
- [34] Saenger, W. Cyclodextrin inclusion compounds in research and industry. *Angew Chem. Int. Ed. Engl.*, **1980**, *19*, 344-362.
- [35] Loftsson, T.; Magnúsdóttir, A.; Masson, M.; Sigurjonsdóttir, J.F. Self-association and cyclodextrin solubilization of drugs. *J. Pharm. Sci.*, **2002**, *91*, 2307-2316.
- [36] Werner, T.C.; Warner, I.M. The use of naphthalene fluorescence probes to study the binding sites on cyclodextrin polymers formed from reaction of cyclodextrin monomers with epichlorohydrin. *J. Inclusion Phenom. Mol. Recogn. Chem.*, **1994**, *18*, 385-396.
- [37] Werner, T.C.; Colwell, K.; Agbaria, R.; Warner, I.M. Binding of pyrene to cyclodextrin polymers. *Appl. Spectrosc.*, **1996**, *50*, 511-516.
- [38] Magnúsdóttir, A.; Masson, M.; Loftsson, T. Self association and cyclodextrin solubilization of NSAIDs. *J. Inclusion Phenom. Macrocycl. Chem.*, **2002**, *44*, 213-218.
- [39] Todorova, N.A.; Schwarz, F.P. The role of water in the thermodynamics of drug binding to cyclodextrin. *J. Chem. Thermodynamics*, **2007**, *39*, 1038-1048.
- [40] Junquera, E.; Aicart, E. Potentiometric study of the encapsulation of ketoprofen by hydroxypropyl- $\beta$ -cyclodextrin. temperature, solvent, and salt effects. *J. Phys. Chem. B*, **1997**, *101*, 7163-7171.
- [41] Mura, P.; Furlanetto, S.; Cirri, M.; Maestrelli, F.; Corti, G.; Pinzauti, S. Interaction of naproxen with ionic cyclodextrins in aqueous solution and in the solid state. *J. Pharm. Biomed. Anal.*, **2005**, *37*, 987-994.
- [42] Wintgens, V.; Amiel, C. New 4-amino-*N*-alkylphthalimides as fluorescence probes for  $\beta$ -cyclodextrin inclusion complexes and hydrophobic microdomains of amphiphilic systems. *J. Photochem. Photobiol., A Chem.*, **2004**, *168*, 217-226.
- [43] Daoud-Mahammed, S.; Couvreur, P.; Gref, R. Novel self-assembling nanogels: Stability and lyophilisation studies. *Int. J. Pharm.*, **2007**, *332*, 185-191.
- [44] Renard, E.; Deratani, A.; Volet, G.; Sebille, B. Preparation and characterization of water soluble high molecular weight  $\beta$ -cyclodextrin-epichlorohydrin polymers. *Eur. Polym. J.*, **1997**, *33*, 49-57.
- [45] Xu, C.; Green, A.; Parisi, A.; Parsons, P.G. Photosensitization of the sunscreen octyl *p*-dimethylaminobenzoate by uva in human melanocytes but not in keratinocytes. *Photochem. Photobiol.*, **2001**, *73*, 600-604.
- [46] Hanson, K.M.; Gratton, E.; Bardeen, C.J. Sunscreen enhancement of UV-induced reactive oxygen species in the skin. *Free Radic. Biol. Med.*, **2006**, *41*, 1205-1212.
- [47] Del Valle, E.M.M. Cyclodextrins and their uses: A review. *Process Biochem.*, **2004**, *39*, 1033-1046.
- [48] Wiggins, P.M. Hydrophobic hydration, hydrophobic forces and protein folding. *Physica A*, **1997**, *238*, 113-128.